

FEA Analysis of TI-6AL-4V and 30% Collagen Reinforced PMC Used as Biomaterials for Ankle Implants

Hemanth B ¹, H G Hanumantharaju ¹ , Prashanth K P ^{2,*} , Sanman S ² , Lavakumar K S ²

¹ Department of Mechanical Engineering, University Visvesvaraya College of Engineering, Bengaluru, India

² Department of Mechanical Engineering, Acharya Institute of Technology, Bengaluru, India

* Correspondence: prashanthkp@acharya.ac.in (P.K.P.);

Scopus Author ID 57200791912

Received: 16.08.2022; Accepted: 19.09.2022; Published: 31.10.2022

Abstract: This paper deals with the feasibility study of using existing biomaterials like titanium alloy and the collagen-reinforced polymer matrix composite for ankle implant application through FEA analysis. The ankle joint is the important joint in the human body that experience maximum compressive stresses and undergoes maximum deformation. It must evaluate properties like stress concentration, deformation zone, and material behavior. The analysis was carried out in ANSYS Workbench with different loading conditions, for instance, normal walking and sprinting. The analysis showed that both the Ti-6Al-4V and the 30% collagen-reinforced PMC exhibited minimum stresses, but since the density of Ti-6Al-4V is more than 30% collagen-reinforced PMC. Even though the stress developed in Ti-6Al-4V is within the yield stress, the density is still not close enough to the density of bone. Collagen-reinforced PMC with a 30% density close to the bone is recommended as an implant material for better life and performance.

Keywords: biomaterials; titanium alloy; collagen; ankle implant; finite element analysis.

© 2022 by the authors. This article is an open-access article distributed under the terms and conditions of the Creative Commons Attribution (CC BY) license (<https://creativecommons.org/licenses/by/4.0/>).

1. Introduction

Ankle sprains in athletes are one of the most widely spread sports injuries, which occurs very often. It is expected that 30-41% of athletes with an ankle sprain may lead to permanent impairments. The usage of advanced material titanium alloy and biomaterials like collagen composites in ankle arthroplasty is gaining interest, mainly due to more functional movements than ankle arthrodesis for the reconstruction of degenerative ankles with end-stage arthritis. After all, medical reports have stated a wide range of iatrogenic complications and a success rate of downfall [1, 2] in ankle procedures. Downrate of success was reported to range from 10% to 20% within 10 years of post-surgery [3-9]. Sometimes failures need conversion to ankle arthrodesis, which may lead to amputation in the worst scenario [10]. Surgical failures might be because prostheses cannot completely mimic normal human ankles, which have complex anatomical components, sophisticated kinematics, and close connections and stability systems. Total ankle arthroplasty biomechanics requires a thorough understanding [11-16]. Previous biomechanical research, such as gait analysis, cadaveric experiments, and radiographic views [17], gave useful but insufficient insight into the inner foot. Computational approaches are utilized to understand human bodies and are commonly used in biomechanical investigations. Finite element (FE) models of Total ankle arthroplasty have been developed and used to investigate the contact pressure and kinematics of the implants during gait. To study the

behavior of biomaterials Ti-6Al-4V and collagen fiber reinforced polymer matrix composite as ankle replacement materials, Finite Element Analysis (FEA) was carried out [18-30]. The ankle joint is an essential joint in the human body subjected to maximum compressive stresses and deformation. Hence it's important to find out the stress concentrations and deformation zones of the implant of the ankle joint.

2. Materials and Method

2.1. Modeling of the implant.

To study the material's behavior, the actual dimensions of the implant are considered. CATIA, as the modeling software 3D model, is created in the part body using all the required 3D options of CATIA. Figure 1 shows the model of the implant.

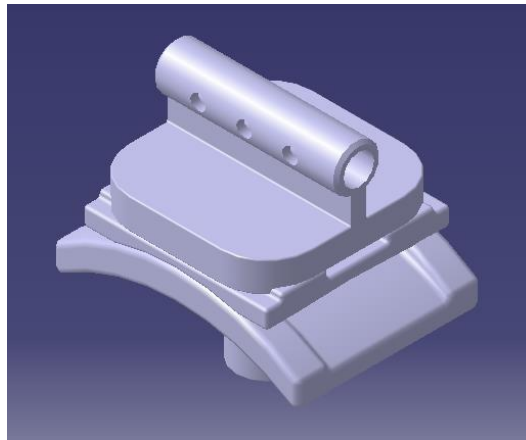


Figure 1. CATIA model of ankle joint implant.

2.2. Finite element model.

The 3D finite element model required for analysis is created by discretizing the geometric model. The discretization was performed in ansys environment. The 3D geometry of the implant was modeled separately. The model is exported as *.stp file. This file is imported into the environment where the implant model is opened. Finally, the model is prepared for analysis. 86,188 elements are created, and triad elements are used. Using ANSYS, different boundary conditions are given, and analysis is performed. Meshed model of the implant is shown in below Figure 2.

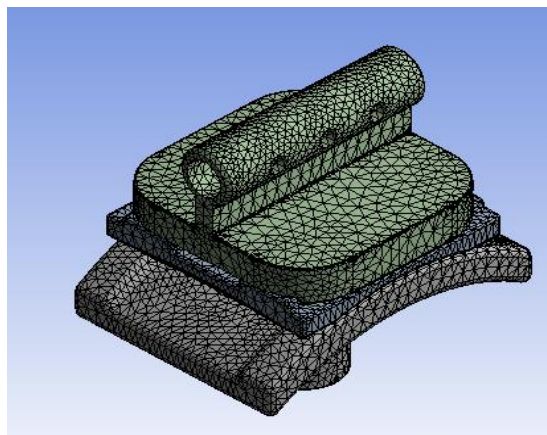


Figure 2. Meshed model.

2.3. Boundary conditions.

For valid results, a FE mesh should be subjected to realistic boundary and loading conditions representative of the actual conditions. For the ankle joint implant analysis, the implant must be free to contact with elements in sliding and radial directions. The implant is fixed at the bottom, similar to the joint inserted in the talus bone. Also, the forces experienced by the ankle joint implant vary greatly under different loading conditions and can reach up to 20 times the body weight while sprinting or jumping. Free body analysis has been utilized to reveal the differences in joint reaction force between single-leg tip-toe stance (3.5-4 times body weight) and single-leg stance under dynamic settings (2.5 times body weight). After showing that the joint reaction force with the foot suspended horizontally in midair is only about 0.02 times the body weight acting in a nearly horizontal direction when compared to the near vertical direction. The magnitude of the joint reaction force in a single stance, the biomechanical justification for maintaining non-weight-bearing status in conservatively managed small posterior malleolus is then presented. The shear force acts between the fibula and talus region. It is estimated to be 80% of the body weight. Figure 3 shows the actual boundary conditions applied to the meshed model.

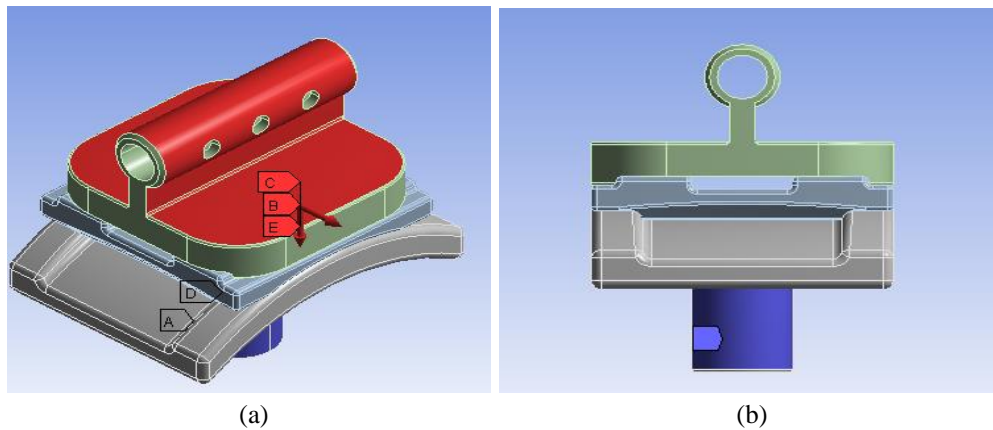


Figure 3. Actual boundary conditions applied to the meshed model (a) Isometric View; (b) Front View.

In this analysis, the maximum load is taken as 4 times the body weight and 80% of the body weight for shear force for the normal walking case. For the jumping or sprinting case maximum load is 20 times the body weight, i.e., impact load. In Figure 3, ‘A’ indicates the model is fixed at the bottom, which is shown in Figure 3 (b). Figure 4 indicates shear acting on the ankle transferred to the implant. D and E is the shear force acting on the implant.

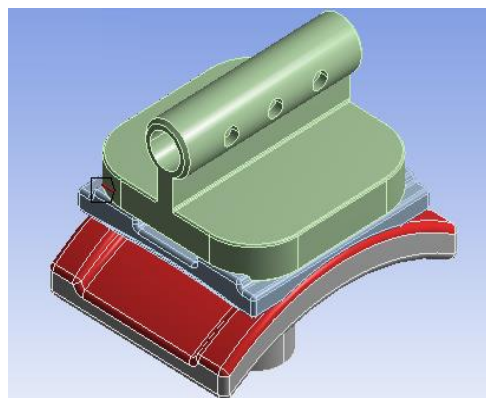


Figure 4. The shear force acting on the ankle, which is transferred to the implant, shown as ‘D’ and ‘E’ in figure 3.

2.4. Numerical analysis.

The finite element analysis is performed to evaluate the stress distribution in the proximal region of ankle replacement implant of Ti-6Al-4V and 30% collagen reinforced PMC under different loading conditions. Since each joint carries a different weight under normal walking and takes heavy loads in sprinting or jumping, analysis is performed for 50kg, 60kg, 70kg, 80kg, 90kg, and 100kg patient weight. The following figures 6 to 29 show the plots of Displacement and Von Misses Stress for materials under normal and impact conditions of 50kg, 60kg, 70kg, 80kg, 90kg, 100 kg patient weight. Each figure shows the maximum and minimum values of displacement and stresses for the material considered. Ti-6Al-4V exhibited maximum stress of 12.912 N/mm² and a maximum displacement of 4.50e⁻⁰⁴mm for the patient body weight of 100kg. Further, Ti-6Al-4V exhibited the maximum stress of 64.6N/mm² and maximum displacement of 2.25x10⁻³ mm for the patient body weight of 100kg under impact loading conditions. Displacement and von misses stresses obtained from analysis for Ti-6Al-4V are shown below in figures 5-16.

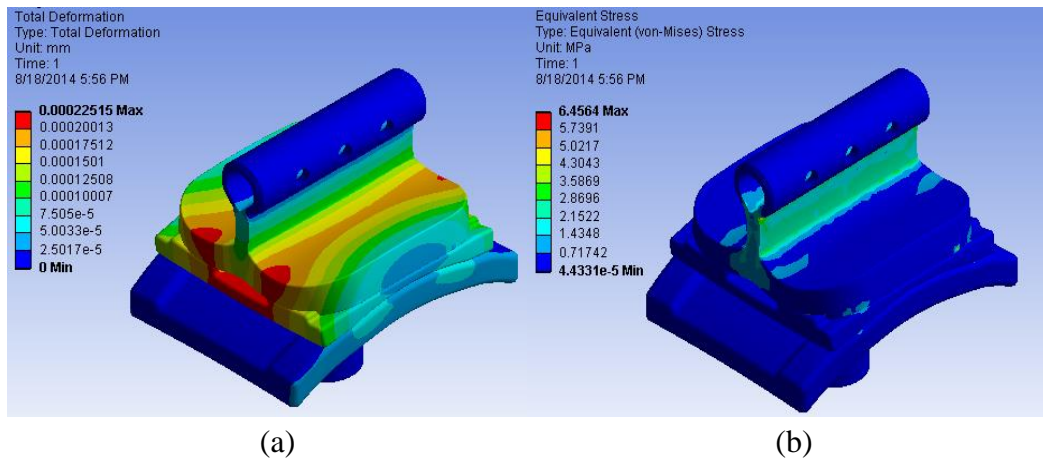


Figure 5. (a) Displacement plot; (b) Von misses stress plot for 50kg Under normal loading(walking) for Ti-6Al-4V.

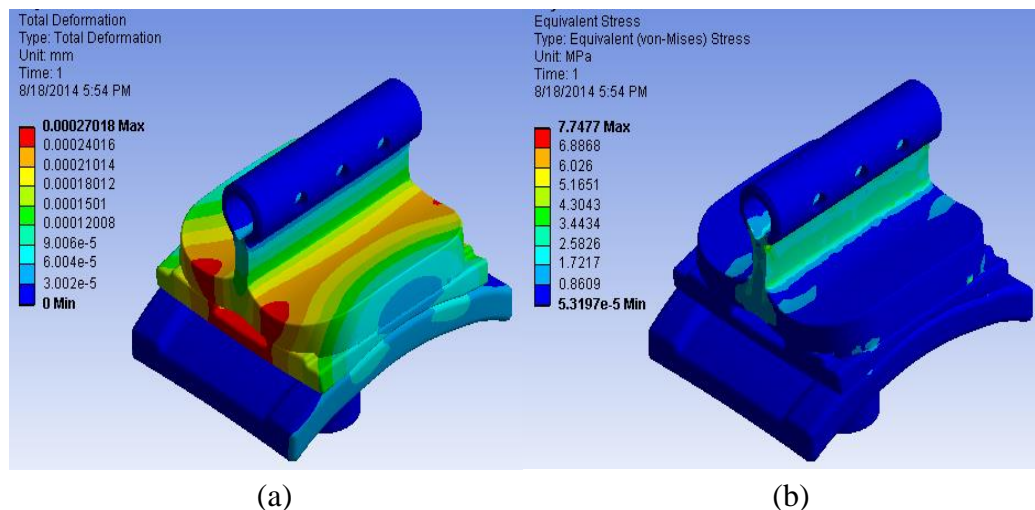


Figure 6. (a) Displacement plot; (b) Von misses stress plot for 60kg Under normal loading(walking) for Ti-6Al-4V.

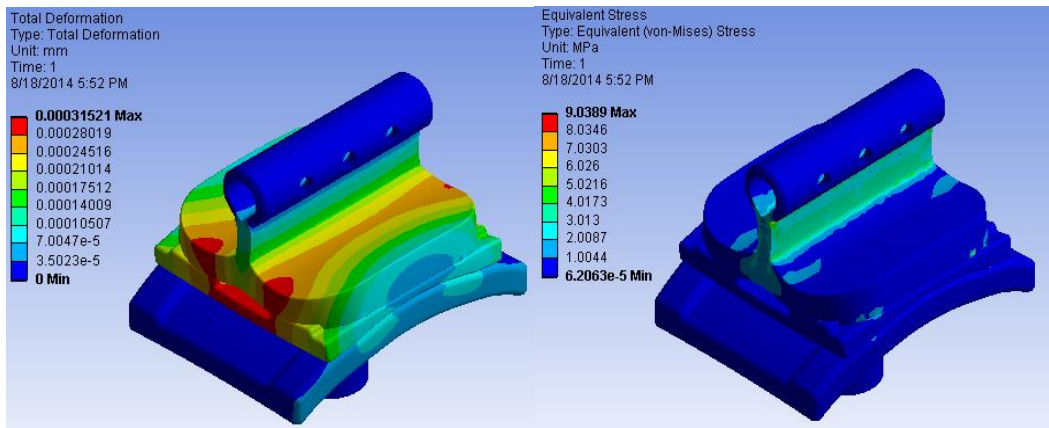


Figure 7. (a) Displacement plot; (b) Von misses stress plot for 70kg Under normal loading(walking) for Ti-6Al-4V.

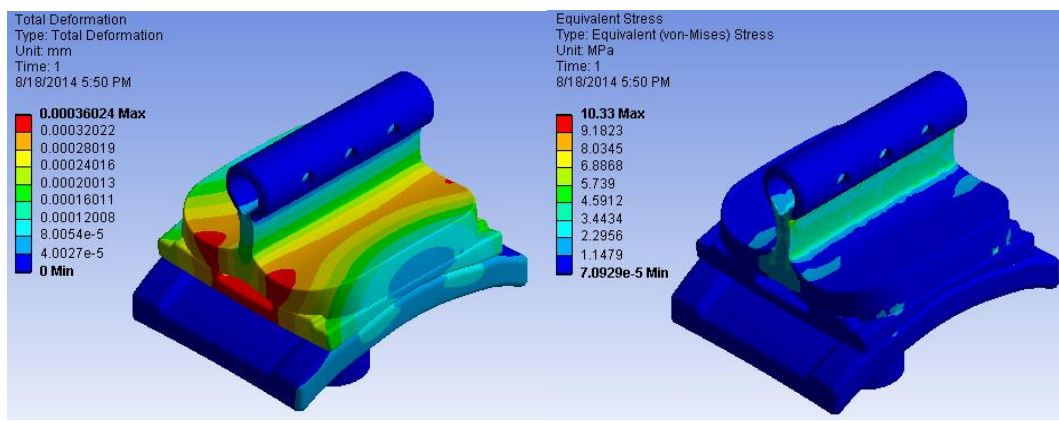


Figure 8. (a) Displacement plot; (b) Von misses stress plot for 80kg Under normal loading(walking) for Ti-6Al-4V.

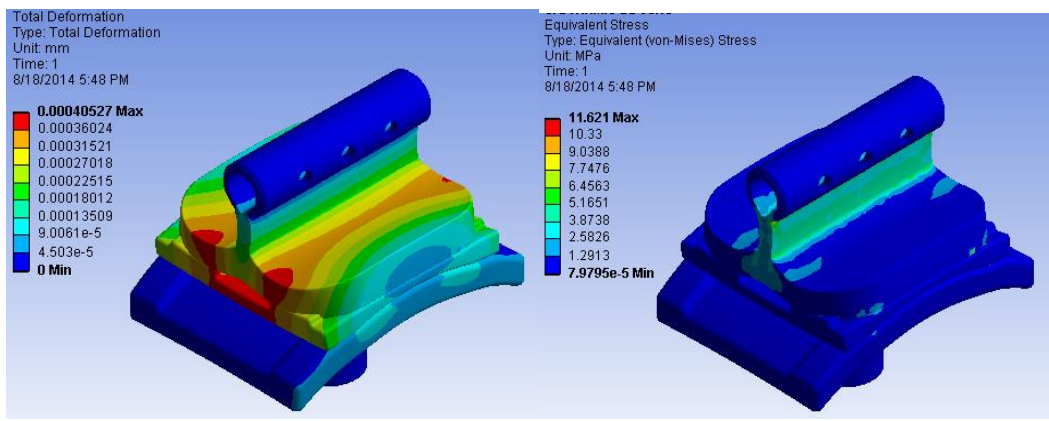


Figure 9. (a) Displacement plot; (b) Von misses stress plot for 90kg Under normal loading(walking) for Ti-6Al-4V.

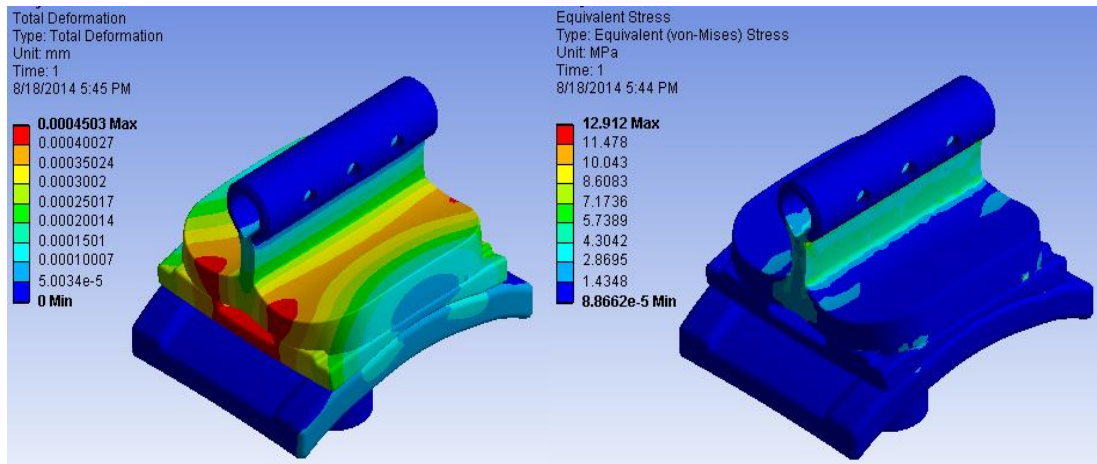


Figure 10. (a) Displacement plot; (b) Von misses stress plot for 100kg Under normal loading(walking) for Ti-6Al-4V.

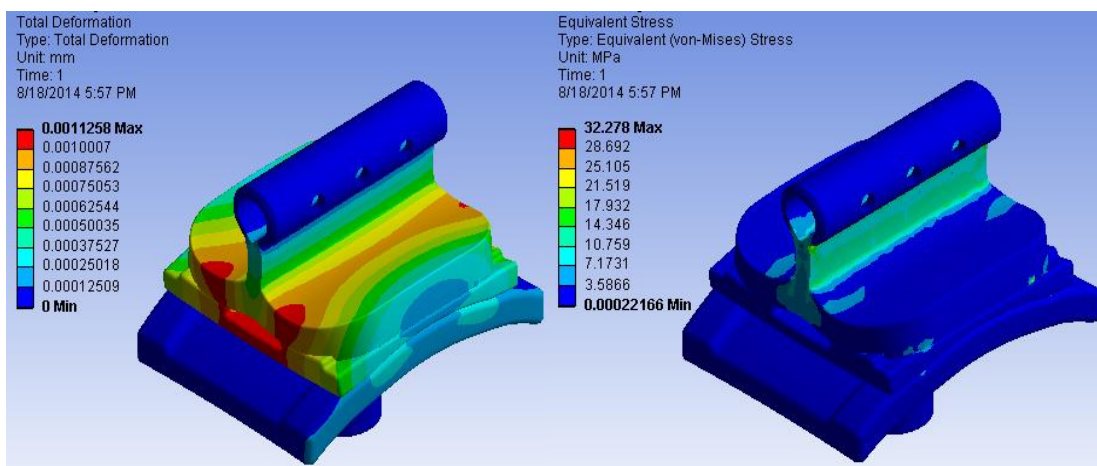


Figure 11. (a) Displacement plot; (b) Von misses stress plot for 50kg Under impact loading for Ti-6Al-4V.

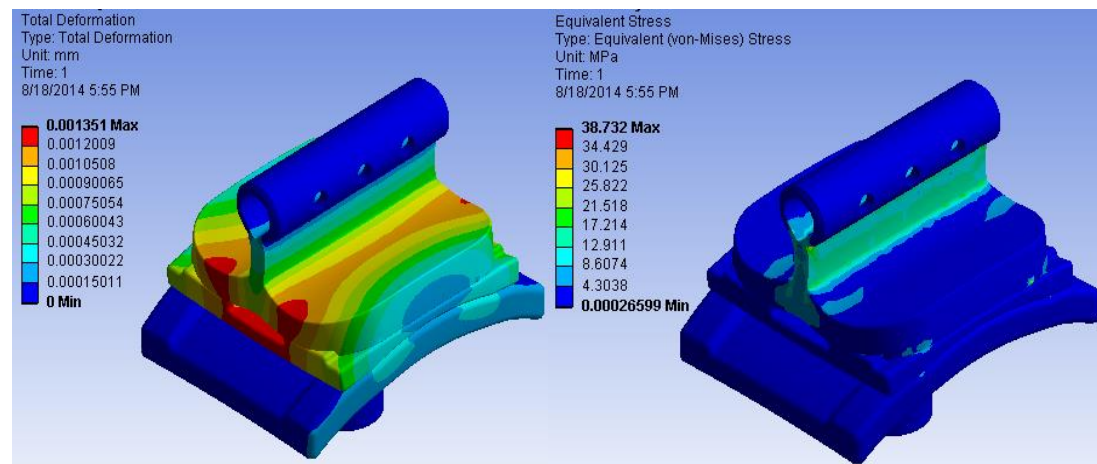


Figure 12. (a) Displacement plot; (b) Von misses stress plot for 60kg Under impact loading for Ti-6Al-4V.

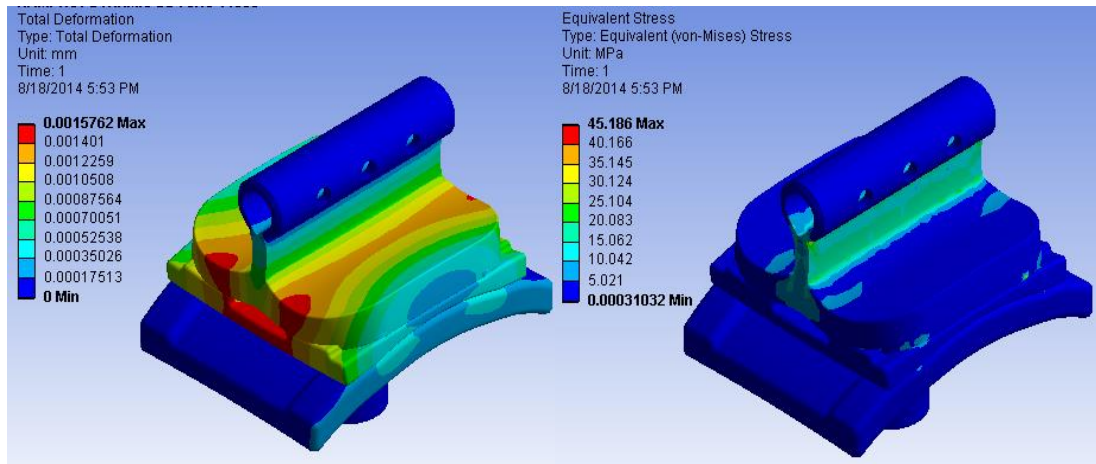


Figure 13. (a) Displacement plot; (b) Von misses stress plot for 70kg Under impact loading for Ti-6Al-4V.

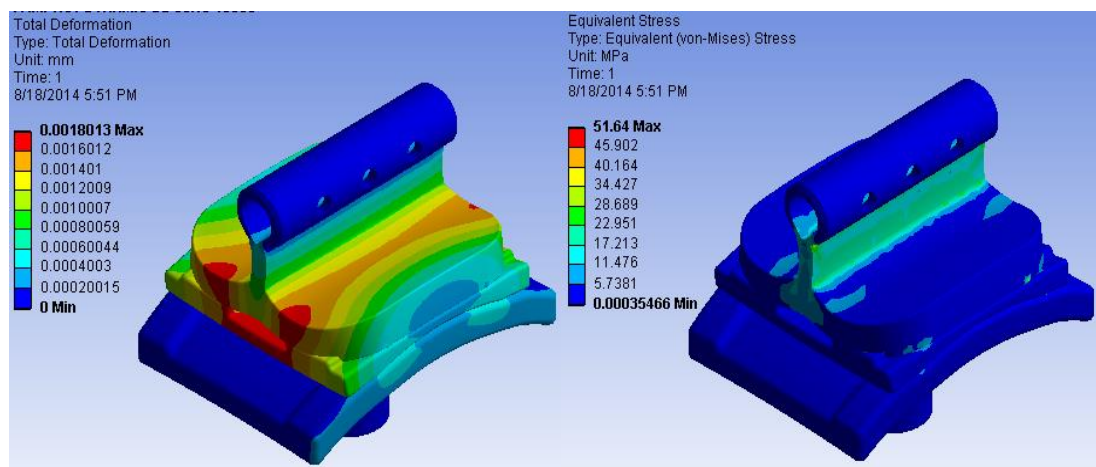


Figure 14. (a) Displacement plot; (b) Von misses stress plot for 80kg Under impact loading for Ti-6Al-4V.

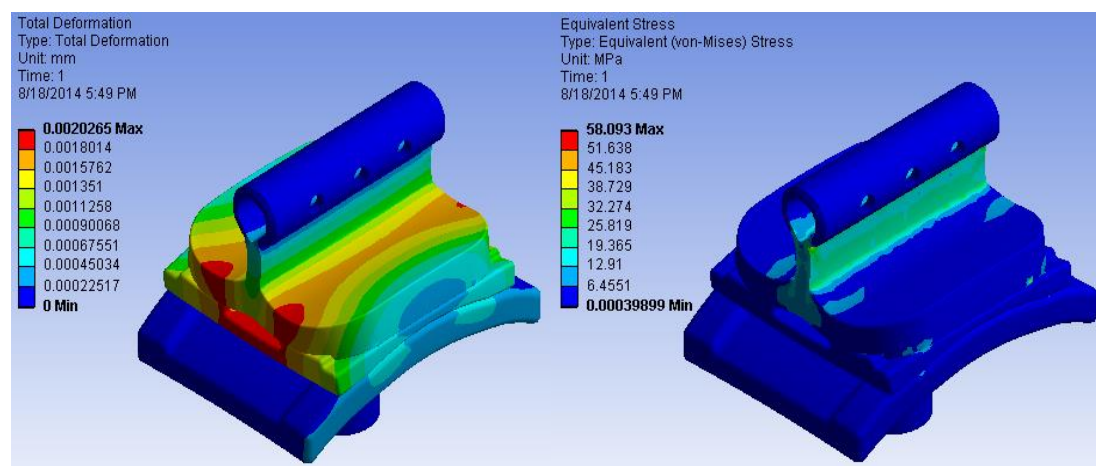


Figure 15. (a) Displacement plot; (b) Von misses stress plot for 90kg Under impact loading.

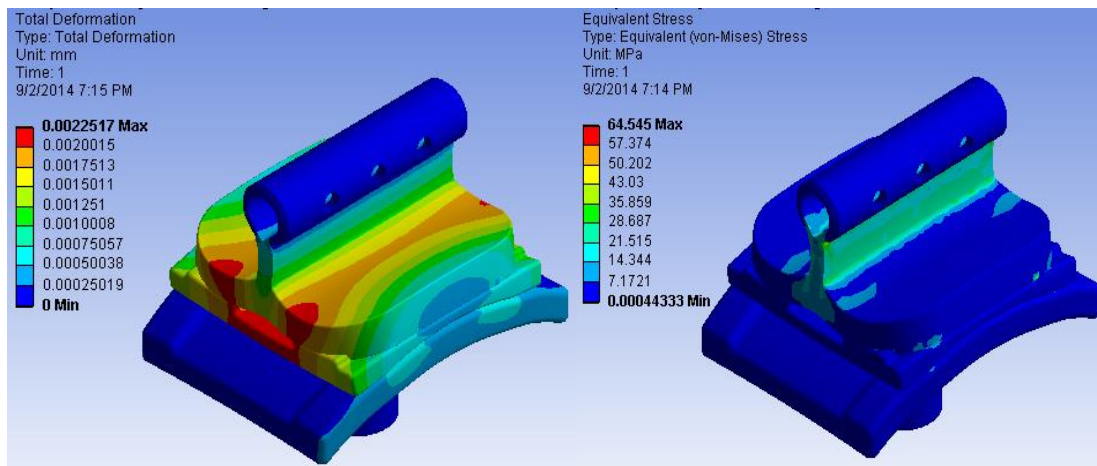


Figure 16. (a) Displacement plot; (b) Von misses stress plot for 100kg Under impact loading for Ti-6Al-4V.

Collagen-reinforced PMC with 30% composition exhibited maximum stress of 14.835 N/mm² and maximum displacement of 6.01e⁻⁰⁴ for the patient body weight of 100kg under normal walking conditions. Further, the said PMC exhibited maximum stress of 74.188 N/mm² and maximum displacement of 3.0097x10⁻⁰³ for the patient body weight of 100kg under impact loading conditions.

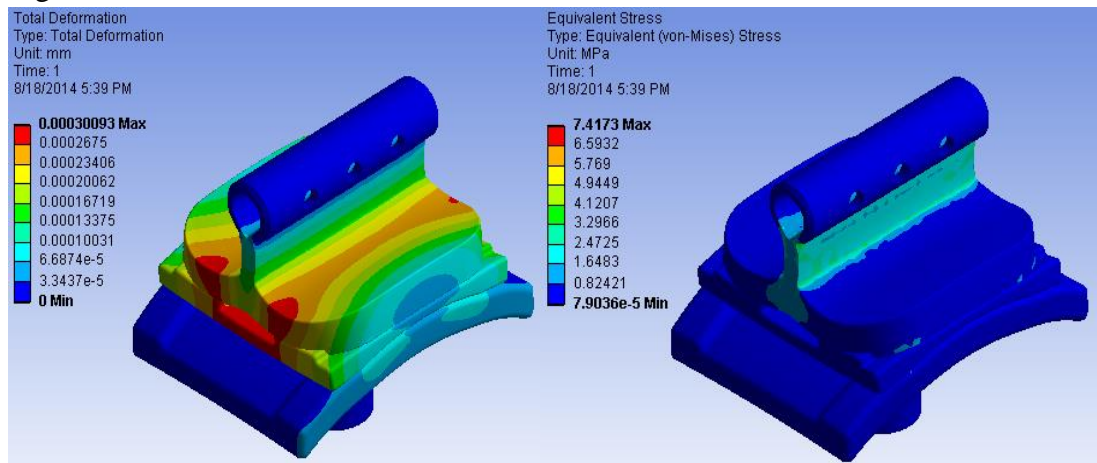


Figure 17. (a) Displacement plot; (b) Von misses stress plot for 50kg Under normal loading(walking) for 30% collagen-reinforced PMC.

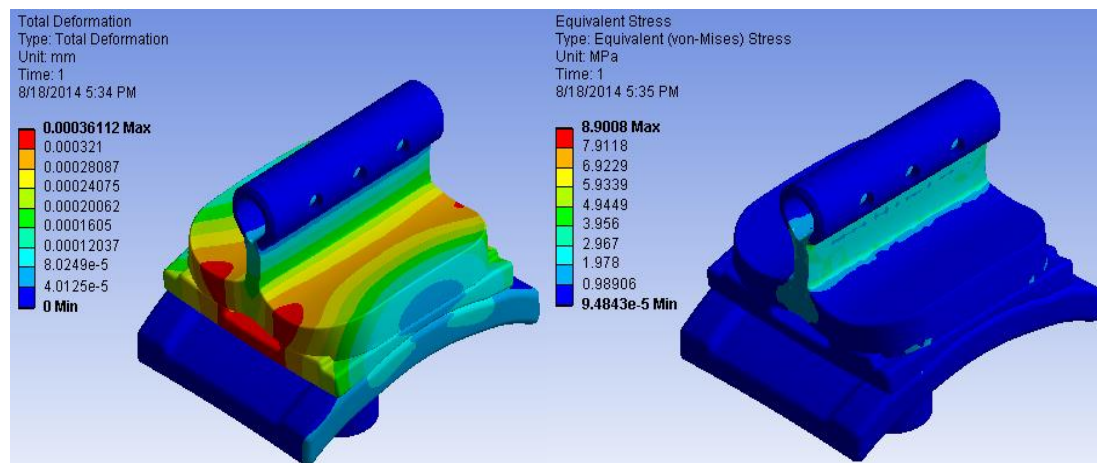


Figure 18. (a) Displacement plot; (b) Von misses stress plot for 60kg Under normal loading(walking) for 30% collagen-reinforced PMC.

The analysis revealed the results which suited for implant materials. However, minimum displacements were observed with reference to the images. It could be further observed that the displacement and stress values varied by the plastic flow of the materials.

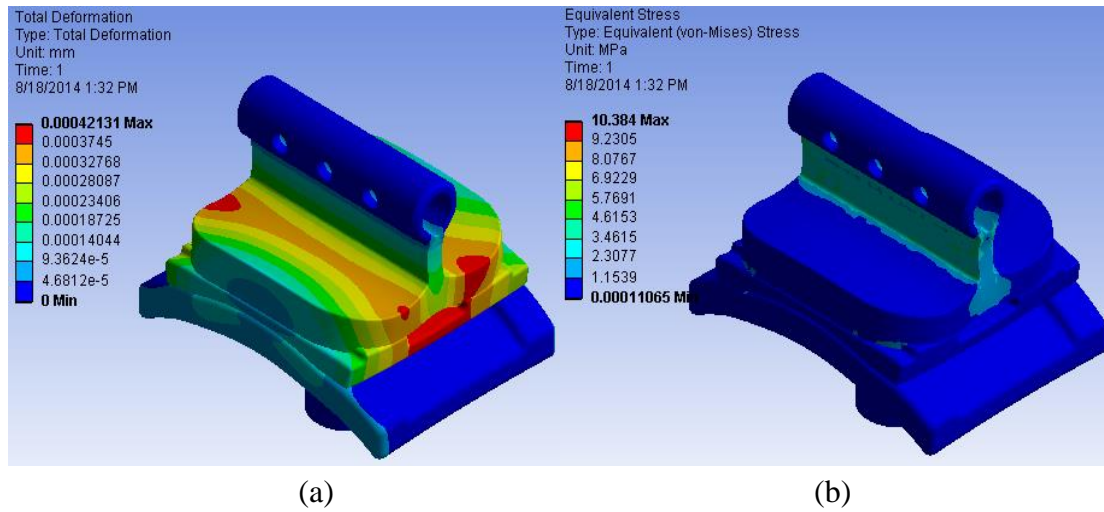


Figure 19. (a) Displacement plot; (b) Von misses stress plot for 70kg Under normal loading(walking) for 30% collagen-reinforced PMC.

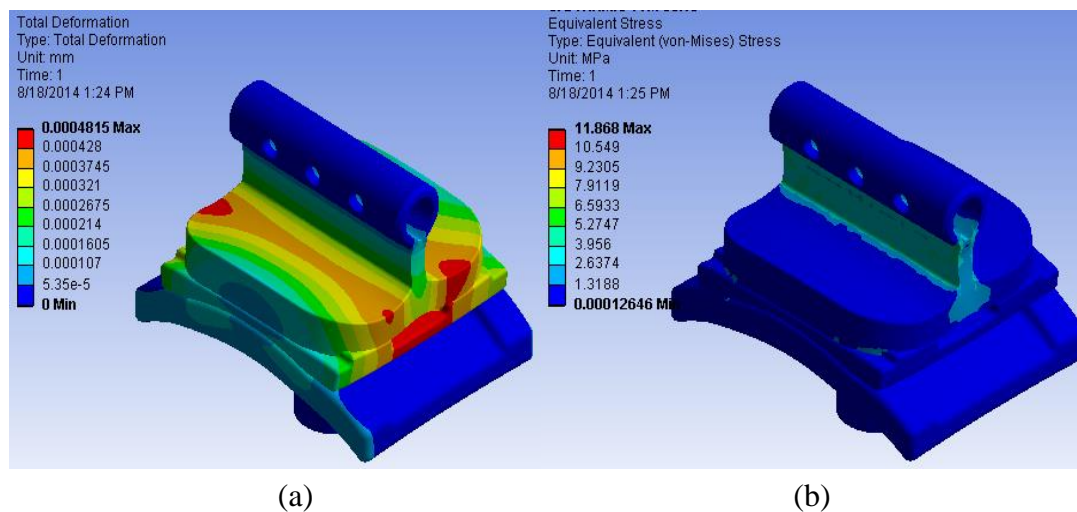


Figure 20. (a) Displacement plot; (b) Von misses stress plot for 80kg Under normal loading(walking) for 30% collagen-reinforced PMC.

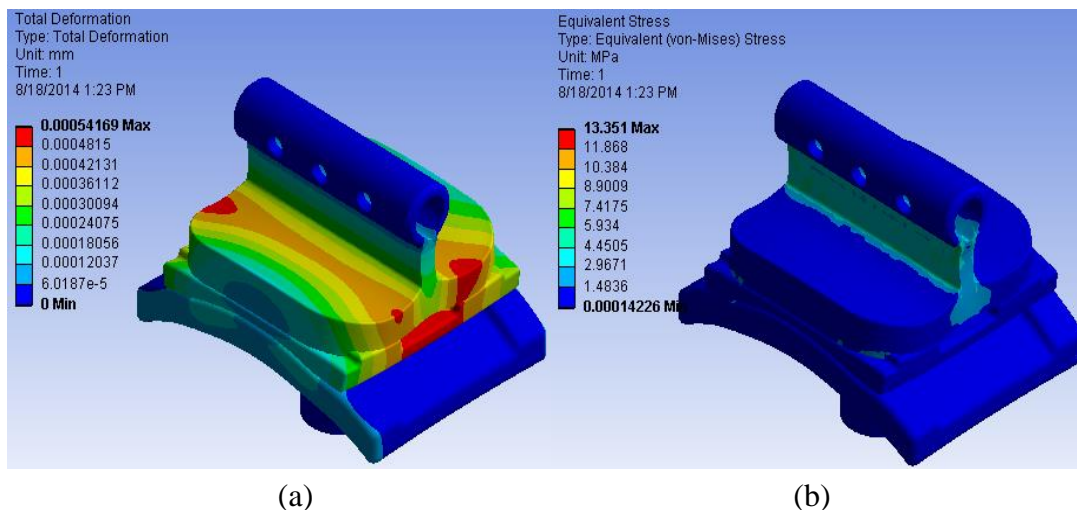


Figure 21. (a) Displacement plot; (b) Von misses stress plot for 90kg Under normal loading(walking) for 30% collagen-reinforced PMC.

Displacement and von misses stresses obtained from analysis for 30% collagen-reinforced PMC is shown below in figures 17-28.

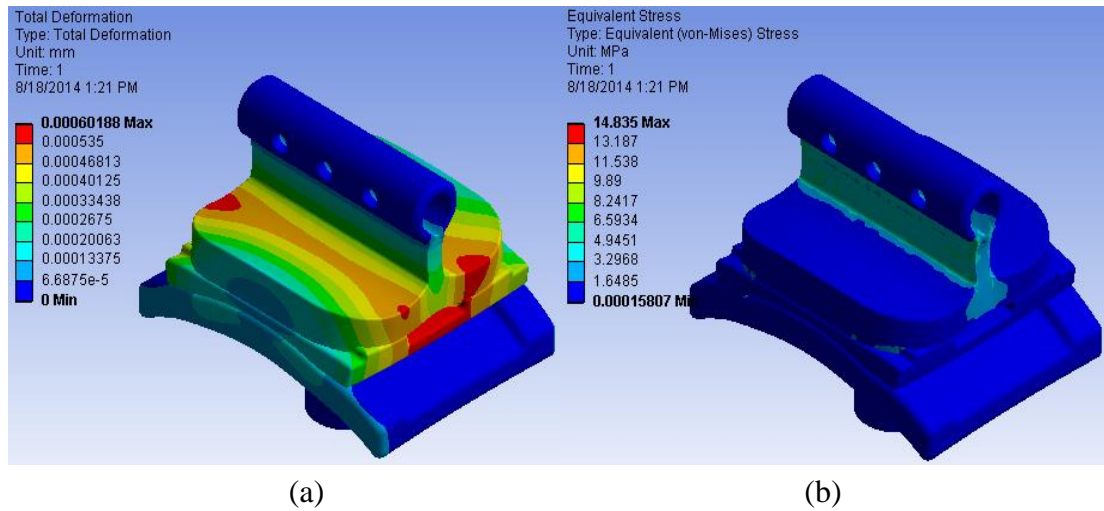


Figure 22. (a) Displacement plot; (b) Von misses stress plot for 100kg Under normal loading(walking) for 30% collagen-reinforced PMC.

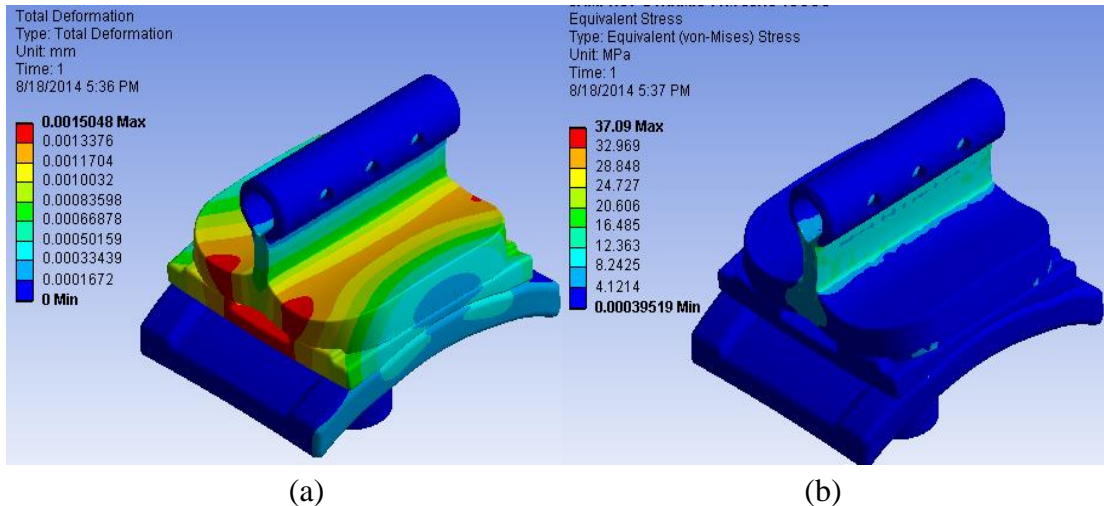


Figure 23. (a) Displacement plot; (b) Von misses stress plot for 50kg Under impact loading for 30% collagen-reinforced PMC.

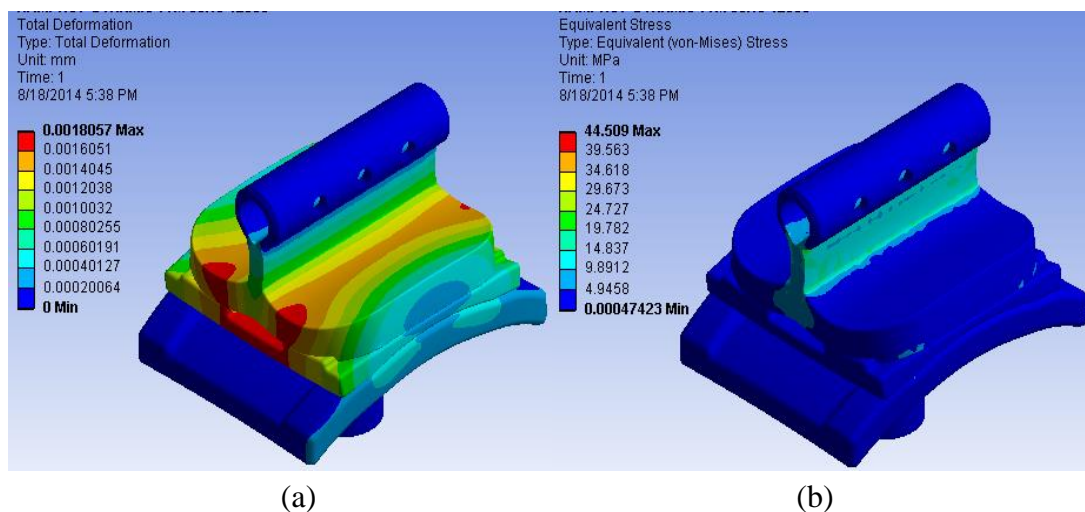


Figure 24. (a) Displacement plot; (b) Von misses stress plot for 60kg Under impact loading for 30% collagen-reinforced PMC.

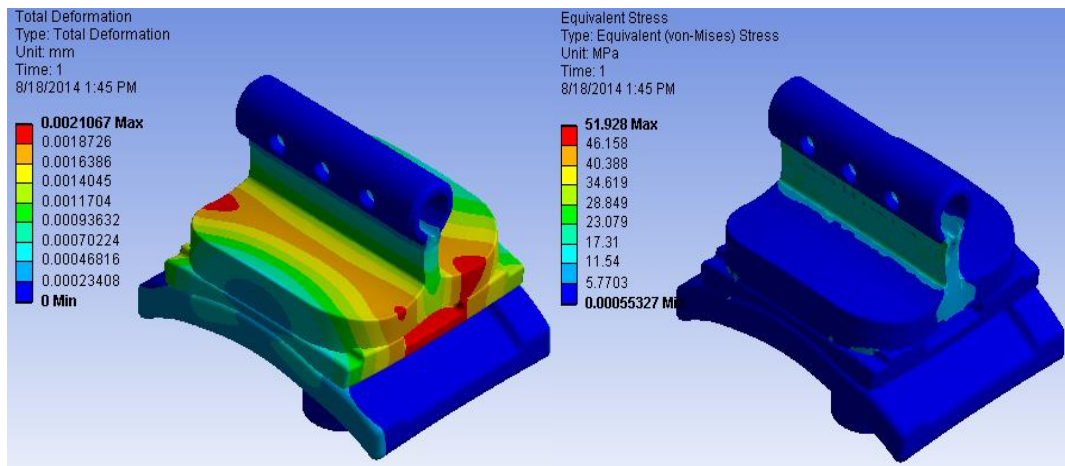


Figure 25. (a) Displacement plot; (b) Von misses stress plot for 70kg Under impact loading for 30% collagen reinforced PMC.

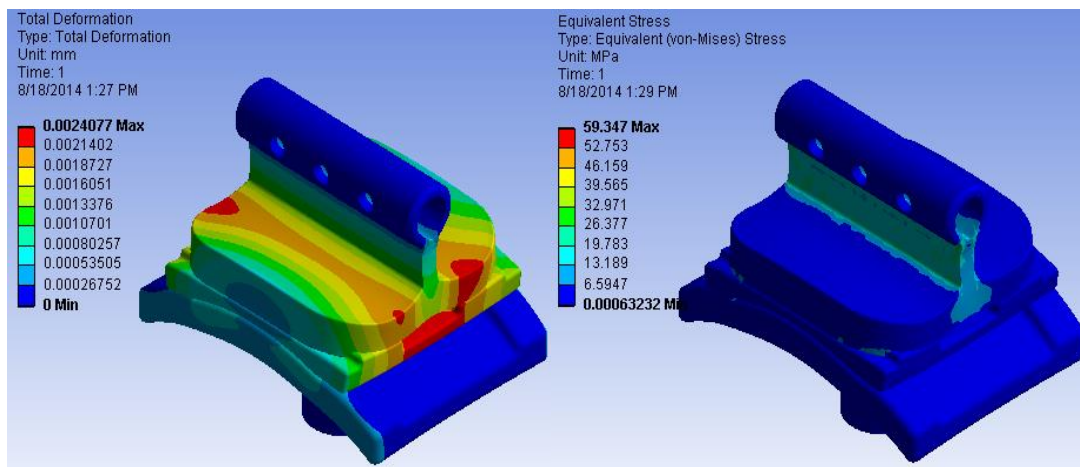


Figure 26. (a) Displacement plot; (b) Von misses stress plot for 80kg Under impact loading for 30% collagen-reinforced PMC.

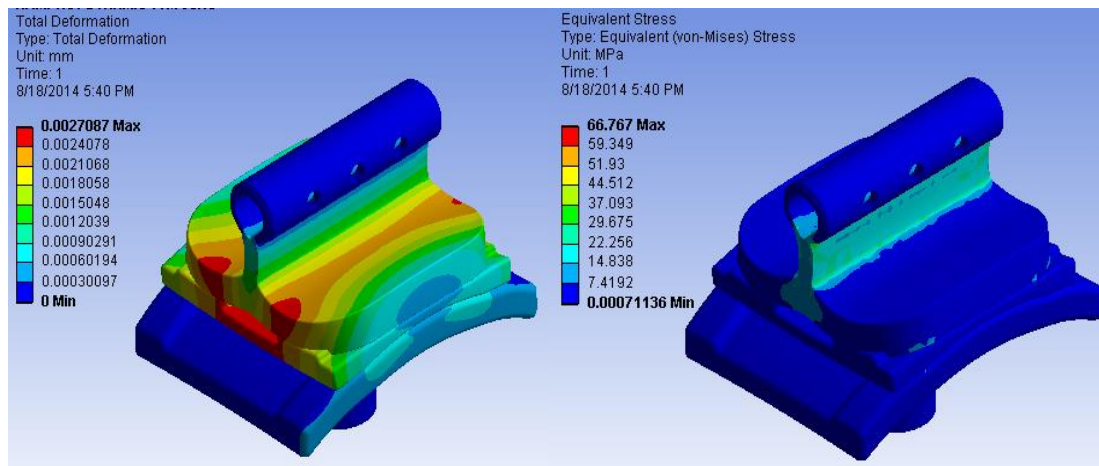


Figure 27. (a) Displacement plot; (b) Von misses stress plot for 90kg Under impact loading for 30% collagen-reinforced PMC.

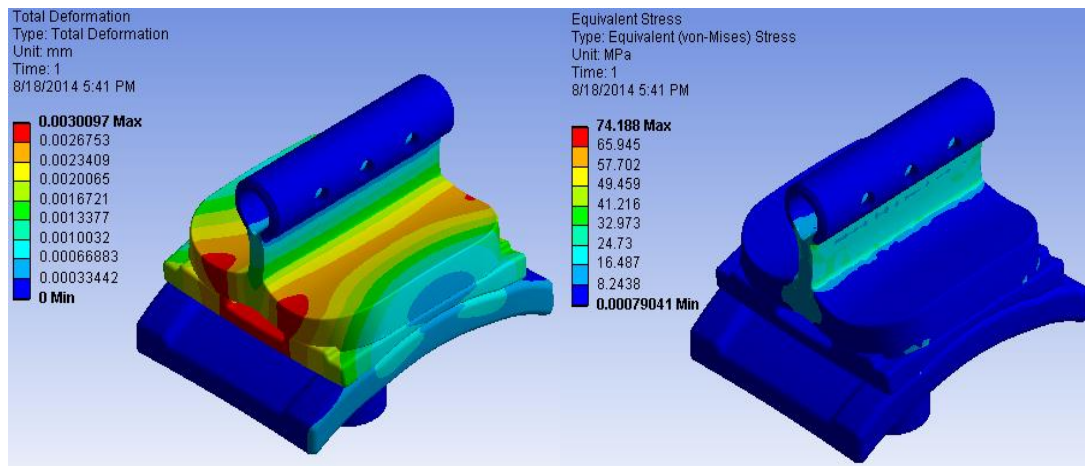


Figure 28. (a) Displacement plot; (b) Von misses stress plot for 100kg Under impact loading for 30% collagen-reinforced PMC.

3. Results and Discussion

Analysis of titanium alloy Ti-6Al-4V and 30% collagen reinforced PMC as ankle joint replacement material under different loading conditions are given in the following table 1 – 4, both for normal loading and for impact loading in terms of displacement and von-misses stresses.

Table 1. Results Summary of Ti-6Al-4V for normal loading condition.

Patient weight (kg)	Maximum Load (N)	Displacement (max) mm	Von misses stress(max)N/mm ²
50	2000	2.25 e ⁻⁰⁴	6.456
60	2400	2.70 e ⁻⁰⁴	7.747
70	2800	3.15 e ⁻⁰⁴	9.038
80	3200	3.60 e ⁻⁰⁴	10.33
90	3600	4.05 e ⁻⁰⁴	11.621
100	4000	4.50 e ⁻⁰⁴	12.912

Table 2. Results Summary of Ti-6Al-4V for impact loading condition.

Patient weight (kg)	Maximum Load (N)	Displacement (max) mm	Von misses stress(max)N/mm ²
50	10000	1.125 e ⁻⁰³	32.278
60	12000	1.35 e ⁻⁰³	38.732
70	14000	1.57 e ⁻⁰³	45.186
80	16000	1.80 e ⁻⁰³	51.64
90	18000	2.02 e ⁻⁰³	58.093
100	20000	2.25 e ⁻⁰³	64.5460

Tables 1, 2, and Figure 29 show the displacement comparison of Ti-6Al-4V for normal and impact load conditions for patient weight in the 50 to 100kg range. It is noticed that during normal load conditions for a load of 2000N, displacement observed is 2.25e⁻⁰⁴mm, and for a load of 4000N, displacement observed is 4.50e⁻⁰⁴mm. Similarly, under impact load conditions, a load of 10000N displacement observed is 1.125e⁻⁰³mm, and a load of 20000N displacement observed is 2.25 e⁻⁰³mm. The results obtained from the present investigation show that with the increase in load, the maximum displacement observed for the material increased.

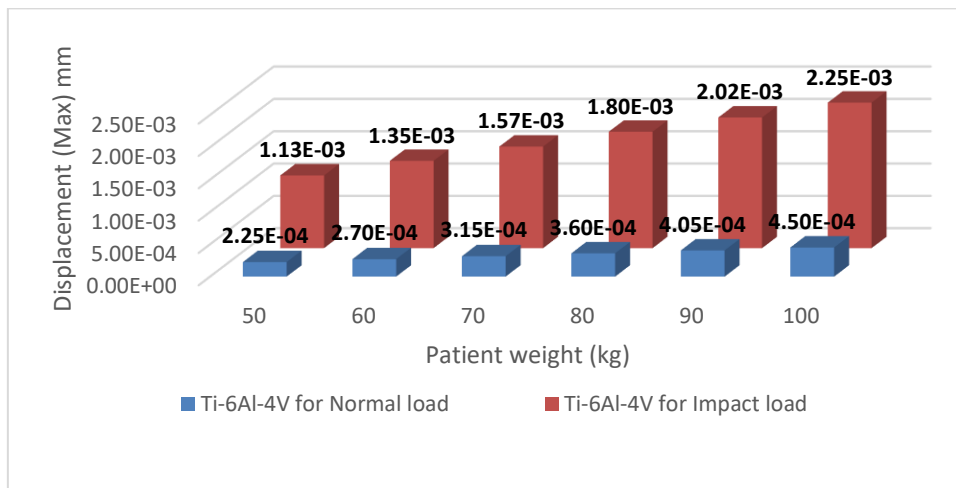


Figure 29. Displacement comparison of Ti-6Al-4V for normal and impact load.

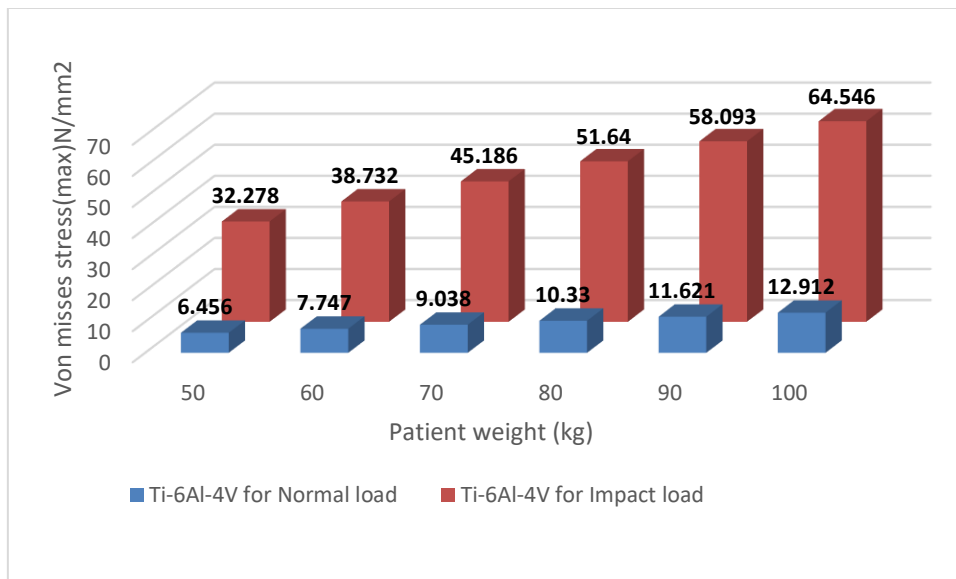


Figure 30. Von misses stress (max) comparison of Ti-6Al-4V for normal and impacts load.

Tables 1, 2, and Figure 30 show the Von misses stress comparison of Ti-6Al-4V for normal and impact load conditions for patient weight in the 50 to 100kg range. It is noticed that during normal load conditions, for the load of 2000N max, Von misses stress observed is 6.456N/mm², and for the load of 4000N, the displacement observed is 12.912 N/mm². Similarly, under impact load conditions, for a load of 10000N, the displacement observed is 32.278N/mm², and for a load of 20000N, the displacement observed is 64.546N/mm². The results obtained from the present investigation show that with the increase in load, the maximum displacement observed for the material increased.

From the above figures, it is observed that Ti-6Al-4V exhibited maximum stress of 12.912 N/mm² and maximum displacement of 4.5e⁻⁰⁴ mm for the patient body weight of 100kg. The stresses produced are within the yield stress; hence the material is safe. Ti-6Al-4V exhibited maximum stress of 64.6 N/mm² and a maximum displacement of 2.25x10⁻⁰³mm for the patient body weight of 100kg.

Table 3. Results summary of 30% collagen-reinforced PMC for normal loading.

Patient weight (kg)	Maximum Load (N)	Displacement (max) mm	Von misses stress(max)N/mm ²
50	2000	3.00 e ⁻⁰⁴	7.4173
60	2400	3.61 e ⁻⁰⁴	8.9008

Patient weight (kg)	Maximum Load (N)	Displacement (max) mm	Von misses stress(max)N/mm ²
70	2800	4.21 e ⁻⁰⁴	10.384
80	3200	4.81 e ⁻⁰⁴	11.868
90	3600	5.41 e ⁻⁰⁴	13.351
100	4000	6.01 e ⁻⁰⁴	14.835

Table 4. Results summary of 30% collagen reinforced PMC for impact load.

Patient weight (kg)	Maximum Load (N)	Displacement (max) mm	Von misses stress(max)N/mm ²
50	10000	1.506 e ⁻⁰³	37.07
60	12000	1.1804 e ⁻⁰³	44.509
70	14000	2.10 e ⁻⁰³	51.928
80	16000	2.40 e ⁻⁰³	59.347
90	18000	2.70 e ⁻⁰³	66.767
100	20000	3.007 e ⁻⁰³	74.188

Tables 3, 4, and Figure 31 show the displacement comparison of 30% collagen-reinforced PMC for normal and impact load conditions for patient weight in the range of 50 to 100kg.

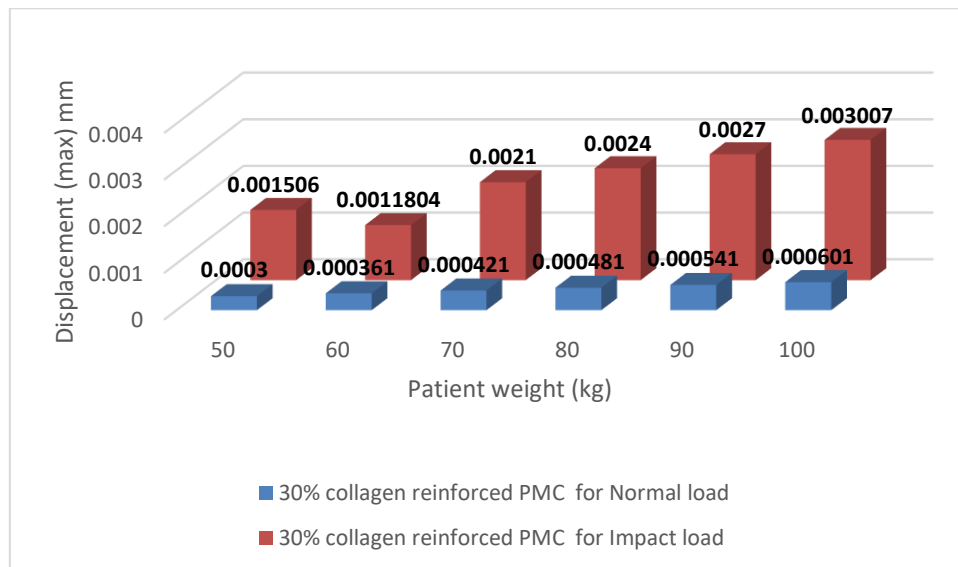


Figure 31. Displacement comparison of 30% collagen-reinforced PMC for normal and impact load.

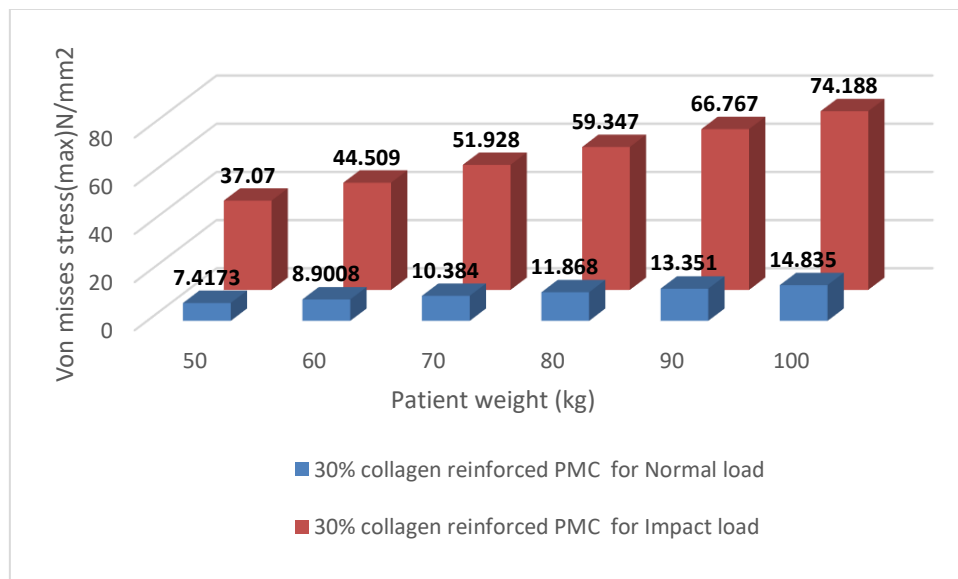


Figure 32. Von misses stress(max) comparison of 30% collagen-reinforced PMC for normal and impacts load.

It is noticed that during normal load conditions for the load of 2000N, displacement observed is $3.00e^{-04}$ mm; for the load of 4000N, displacement observed is $1.506 e^{-03}$ mm. Similarly, under impact load conditions, for a load of 10000N, the displacement observed is $1.125e^{-03}$ mm, and for a load of 20000N, the displacement observed is $3.007e^{-03}$ mm. The results obtained from the present investigation show that with the increase in load, the maximum displacement observed for the material increased.

Tables 3, 4, and Figure 32 show the Von misses stress comparison of 30% collagen-reinforced PMC for normal and impact load conditions for patient weight in the range of 50 to 100kg. It is noticed that during normal load conditions, for the load of 2000N max Von misses stress observed is $7.4173N/mm^2$, and for the load of 4000N, the displacement observed is $14.835N/mm^2$. Similarly, under impact load conditions, for a load of 10000N, the displacement observed is $37.07N/mm^2$ and for a load of 20000N, the displacement observed is $74.188N/mm^2$. The results obtained from the present investigation show that with the increase in load, the maximum Von misses stress observed for the material increased.

From the charts, it is observed that 30% collagen-reinforced PMC exhibited maximum stress of $14.835 N/mm^2$ and maximum displacement of $6.01e^{-04}$ for the patient body weight of 100kg under normal walking conditions. The stresses produced are within the yield stress. 30% collagen-reinforced PMC exhibited maximum stress of $74.188 N/mm^2$ and maximum displacement of 3.009×10^{-03} mm for the patient body weight of 100kg under impact loading conditions. The stresses produced are within the yield stress.

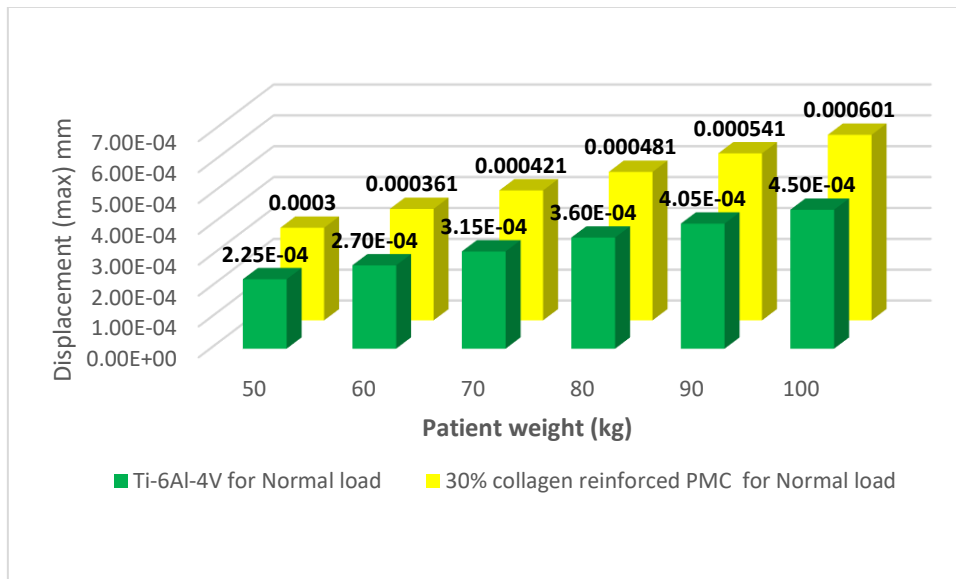


Figure 33. Displacement comparison of Ti-6Al-4V and 30% collagen-reinforced PMC for a normal load.

Figure 33 shows the displacement comparison of Ti-6Al-4V and 30% collagen-reinforced PMC for normal and impact load conditions for patient weight in the range of 50 to 100kg. The chart shows that with an increase in load, the displacement of both materials is increasing. It is noticed that 30% collagen-reinforced PMC showed better displacement than the Ti-6Al-4V alloy for the same loading conditions. Thus, 30% collagen-reinforced PMC is a better ductile property when compared with Ti-6Al-4V alloy. However, since displacement is marginal for the applied load, both materials showed exceptionally acceptable limits for ankle implants.

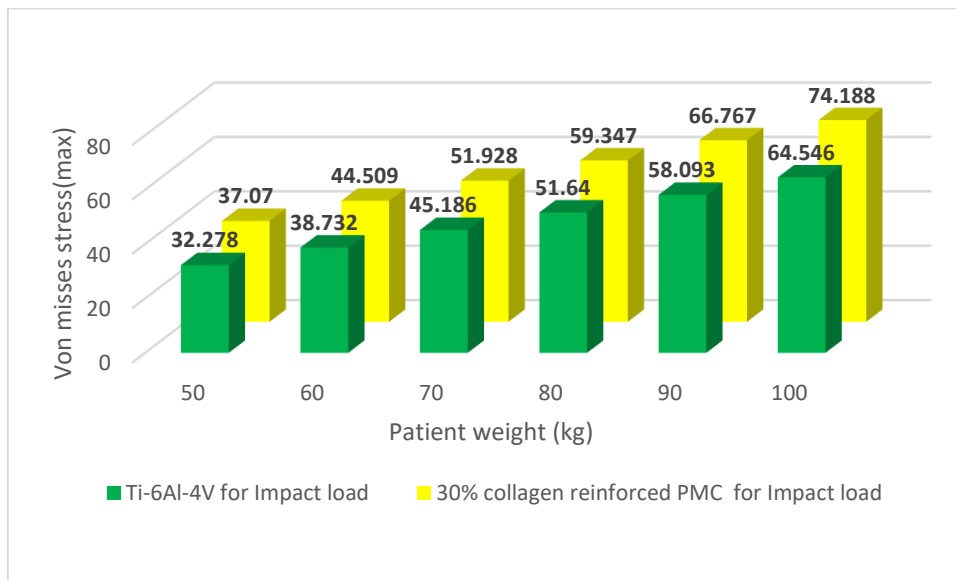


Figure 34. Von misses stress(max) comparison of Ti-6Al-4V and 30% collagen-reinforced PMC for a normal load.

Figure 34 shows the Von misses stress comparison of Ti-6Al-4V and 30% collagen-reinforced PMC for normal and impact load conditions for patient weight in the range of 50 to 100kg. The chart shows that with an increase in load, Von misses stress of both the material is increasing. It is noticed that 30% collagen-reinforced PMC shows higher Von misses stress than the Ti-6Al-4V alloy for the same loading conditions. Thus, 30% collagen-reinforced PMC provides a better stress state that exceeds the yield stress obtained from a uniaxial tensile test for ankle implants compared to Ti-6Al-4V alloy.

4. Conclusions

The 3D finite element model required for analysis is created by discretizing the geometric model. 86,188 elements were created using triad elements. To get valid results, FE mesh is subjected to realistic boundary and loading conditions that replicate the actual conditions. In this analysis, the maximum load is considered as 4 times the body weight, and shear force is taken 80% of the body weight for normal walking. While jumping or sprinting maximum load is considered to be 20 times the body weight. The model is fixed at the bottom, and the load was applied vertically as compressive loading. Von Misses stress and displacement values in the implant were calculated. The analysis results showed that both the Ti-6Al-4V and the 30% collagen-reinforced PMC showed minimum stresses but since the density of Ti-6Al-4V is more compared to 30% collagen-reinforced PMC. Even though the stress developed in Ti-6Al-4V is within the yield stress, the density is still not close enough to the density of bone. The analysis shows that titanium alloy (Ti-6Al-4V) has minimum stresses and high density compared to the collagen-reinforced polymer matrix composite (PMC). As Ti-6Al-4Valloy is heavier in density, it is not compatible with the bone. Thus, a person can feel the presence of an implant in the body. Also, all the metal/metal alloys are denser than bone, thus lacking compatibility with the bone. Therefore, collagen-reinforced PMC with a 30% composition having a density close to that of bone is recommended as an implant material for better life and performance.

Funding

This research received no external funding.

Acknowledgments

This research has no acknowledgment.

Conflicts of Interest

The authors declare no conflict of interest.

Reference

1. Spirt, AA.; Assal, M.; Hansen, S.T.Jr. Complications and failure after total ankle arthroplasty. *J Bone Joint Surg Am.* **2004**, *86*, 1172-1178, <https://doi.org/10.2106/00004623-200406000-00008>.
2. Criswell, B.J.; Douglas, K.; Naik, R.; Thomson, A.B. High revision and reoperation rates using the Agility™ Total Ankle System. *Clin Orthop Relat Res.* **2012**, *470*, 1980-1986, <https://doi.org/10.1007/s11999-012-2242-6>.
3. Knecht, S.I.; Estin, M.; Callaghan, J.J.; Zimmerman, M.B.; Alliman, K.J.; Alvine, F.G.; Saltzman, C.L. The Agility total ankle arthroplasty. Seven to sixteen-year follow-up. *J Bone Joint Surg Am.* **2004**, *86*, 1161-1171, <https://pubmed.ncbi.nlm.nih.gov/15173288/>.
4. Henricson, A.; Skoog, A.; Carlsson, A. The Swedish Ankle Arthroplasty Register: An analysis of 531 arthroplasties between 1993 and 2005. *Acta Orthop.* **2007**, *78*, 569-574, <https://doi.org/10.1080/17453670710014248>.
5. Gougoulias, N.; Khanna, A.; Maffulli, N. How successful are current ankle replacements?: a systematic review of the literature. *Clin Orthop Relat Res.* **2010**, *468*, 199-208, <https://doi.org/10.1007/s11999-009-0987-3>.
6. Karantana, A.; Hobson, S.; Dhar, S. The scandinavian total ankle replacement: survivorship at 5 and 8 years comparable to other series. *Clin Orthop Relat Res.* **2010**, *468*, 951-957, <https://doi.org/10.1007/s11999-009-0971-y>.
7. Wood, P.L.; Karski, M.T.; Watmough, P. Total ankle replacement: the results of 100 mobility total ankle replacements. *The Journal of bone and joint surgery* **2010**, *92B*, <https://doi.org/10.1302/0301-620X.92B7.23852>.
8. Bonnin, M.; Gaudot, F.; Laurent, J.R.; Ellis, S.; Colombier, J.A.; Judet, T. The Salto total ankle arthroplasty: survivorship and analysis of failures at 7 to 11 years. *Clinical Orthopaedics and Related Research* **2011**, *469*, 225-236, <https://doi.org/10.1007/s11999-010-1453-y>.
9. Hsu, A.R.; Haddad, S.L.; Myerson, M.S. Evaluation and management of the painful total ankle arthroplasty. *J Am Acad Orthop Surg.* **2015**, *23*, 272-282, <https://doi.org/10.5435/JAAOS-D-14-00017>.
10. Haddad, S.L.; Coetzee, J.C.; Estok, R.; Fahrbach, K.; Banel, D.; Nalysnyk, L. Intermediate and long-term outcomes of total ankle arthroplasty and ankle arthrodesis. A systematic review of the literature. *J Bone Joint Surg Am.* **2007**, *89*, 1899-1905, <https://doi.org/10.2106/JBJS.F.01149>.
11. Goncalves, A.D.; Balestri, W.; Reinwald, Y. Biomedical Implants for Regenerative Therapies. In: *Vizureanu, P.; Da Cunha Ferreira Botelho, C.M. (Eds.), Biomaterials* **2020**, IntechOpen, <https://doi.org/10.5772/intechopen.91295>.
12. Mazzotti, A.; Arceri, A.; Zielli, S.; Bonelli, S.; Viglione, V.; Faldini, C. Patient-specific instrumentation in total ankle arthroplasty. *World J Orthop.* **2022**, *13*, 230-237, <https://doi.org/10.5312/wjo.v13.i3.230>.
13. Deleu, P.A.; Naaim, A.; Chèze, L. et al. Decreased Mechanical Work Demand in the Chopart Joint After Total Ankle Replacement. *Foot & Ankle International* **2022**, *43*, 1354-1363, <https://doi.org/10.1177/10711007221112094>.
14. Lin, J.; Sofka, C.M.; Demetracopoulos, C.A.; Potter, H.G. The Utility of Isotropic 3D Magnetic Resonance Imaging in Assessing Painful Total Ankle Replacements. *Foot & Ankle Orthopaedics* **2022**, *7*, 1-10, <https://doi.org/10.1177/24730114221094840>.
15. Patil, V.; Balivada, S.; Appagana, S. Biomedical Applications of Titanium and Aluminium Based High Entropy Alloys. *International Journal of Health Technology and Innovation* **2022**, *1*.

16. Jastifer, J.; Coughlin M.J.; Hirose, C. Performance of total ankle arthroplasty and ankle arthrodesis on uneven surfaces, stairs, and inclines: a prospective study. *Foot Ankle Int.* **2015**, *36*, 11-17, <https://doi.org/10.1177/1071100714549190>.
17. Sarraf, M.; Rezvani Ghomi, E.; Alipour, S. et al. A state-of-the-art review of the fabrication and characteristics of titanium and its alloys for biomedical applications. *Biodes. Manuf.* **2022**, *5*, 371-395, <https://doi.org/10.1007/s42242-021-00170-3>.
18. Pradeep, N.B.; Rajath Hegde, M.M.; Manjunath Patel, G.C.; Giasin, K.; Pimenov, D.Y.; Wojciechowski, S. Synthesis and characterization of mechanically alloyed nanostructured ternary titanium based alloy for biomedical applications. *Journal of Materials Research and Technology*, **2022**, *16*, 88-101, <https://doi.org/10.1016/j.jmrt.2021.11.101>.
19. Khosravi, F.; Khorasani, S.N.; Khalili, S. et al. Development of a Highly Proliferated Bilayer Coating on 316L Stainless Steel Implants. *Polymers* **2020**, *12*, 1022, <https://doi.org/10.3390/polym12051022>.
20. Pradeep, N.B.; Venkatesha, B.K.; Parameshwara, S.; Raghavendra Rao, R.; Raviprakash, M. Synthesis of nanostructured ternary Ti based alloy for bio-medical applications. *Materials Today: Proceedings* **2022**, *54*, 372-377, <https://doi.org/10.1016/j.matpr.2021.09.429>.
21. Fu, Y.; Xiao, W.L.; Wang, J.S. et al. A novel strategy for developing $\alpha+\beta$ dual-phase titanium alloys with low Young's modulus and high yield strength. *Journal of Material Science & Technology* **2021**, *76*, 122-128, <https://doi.org/10.1016/j.jmst.2020.11.018>.
22. Sing, S.L. Perspectives on Additive Manufacturing Enabled Beta-Titanium Alloys for Biomedical Applications. *Int J Bioprint.* **2022**, *8*, 478, <http://dx.doi.org/10.18063/ijb.v8i1.478>.
23. Bains, P.S.; Bahraminasab, M.; Sidhu, S.S., Singh, G. On the machinability and properties of Ti-6Al-4V biomaterial with n-HAp powder-mixed ED machining. *Proceedings of the Institution of Mechanical Engineers, Part H: Journal of Engineering in Medicine* **2020**, *234*, 232-242, <https://doi.org/10.1177/0954411919891887>.
24. Benea, L.; Simionescu-Bogatu, N. Reactivity and Corrosion Behaviors of Ti6Al4V Alloy Implant Biomaterial under Metabolic Perturbation Conditions in Physiological Solutions. *Materials* **2021**, *14*, 7404, <https://doi.org/10.3390/ma14237404>.
25. Hemanth, B.; Hanumantharaju, H.B.; Prashanth, K.P.; Venkatesha, B.K. Investigation of wear characteristics of collagen fiber reinforced polymer matrix composites used for orthopaedic implants. *Materials Today: Proceedings* **2022**, *54*, 498-501, <https://doi.org/10.1016/j.matpr.2021.11.429>.
26. Chen, X.; Mao, B.; Zhu, Z. et al. A three-dimensional finite element analysis of mechanical function for 4 removable partial denture designs with 3 framework materials: CoCr, Ti-6Al-4V alloy and PEEK. *Sci Rep* **2019**, *9*, 13975, <https://doi.org/10.1038/s41598-019-50363-1>.
27. Yu, J.; Zhao, D.; Chen, W.M. et al. Finite element stress analysis of the bearing component and bone resected surfaces for total ankle replacement with different implant material combinations. *BMC Musculoskelet Disord* **2022**, *23*, 70, <https://doi.org/10.1186/s12891-021-04982-3>.
28. Bejjani, R.; Salame, C.; Olsson, M. An Experimental and Finite Element Approach for a Better Understanding of Ti-6Al-4V Behavior When Machining under Cryogenic Environment. *Materials* **2021**, *14*, 2796, <https://doi.org/10.3390/ma14112796>.
29. Natsakis, T.; Burg, J.; Dereymaeker, G.; Vander Sloten, J.; Jonkers, I. Extrinsic Muscle Forces Affect Ankle Loading Before and After Total Ankle Arthroplasty. *Clin Orthop Relat Res.* **2015**, *473*, 3028-3037, <https://doi.org/10.1007%2Fs11999-015-4346-2>.
30. Prashanth, K.P.; Hanumantharaju, H.G. Characterization and Analysis of Polymers Used as Artificial Skin, *Materials Today: Proceedings* **2018**, *5*, 2488-2495, <https://doi.org/10.1016/j.matpr.2017.11.030>.